Physical properties and stratigraphy of surface snow in western Dronning Maud Land, Antarctica

Eija Kärkäs, Tõnu Martma & Eloni Sonninen

Information about the spatial variations of snow properties and of annual accumulation on ice sheets is important if we are to understand the results obtained from ice cores, satellite remote sensing data and changes in climate patterns. The layer structure and spatial variations of physical properties of surface snow in western Dronning Maud Land were analysed during the austral summers 1999/2000, 2000/01 and 2003/04 in five different snow zones. The measurements were performed in shallow (1 - 2 m) snow pits along a transect extending 350 km from the seaward edge of the ice shelf to the polar plateau. These pits covered at least the last annual accumulation and ranged in elevation from near sea level to 2500 m a.s.l. The $\delta^{18}O$ values and accumulation rates had a good linear correlation with the distance from the coast. The mean accumulation on the ice shelf was 312 ± 28 mm water equivalent (w.e.); in the coastal region it was 215 ± 43 mm w.e. and on the polar plateau it was 92 ± 25 mm w.e. The mean annual conductivity and grain size values decreased exponentially with increasing distance from the ice edge, by 48 %/100 km and 18 %/100 km respectively. The mean grain size varied between 1.5 and 1.8 mm. Depth hoar layers were a common phenomenon, especially under thin ice crusts, and were associated with low dielectric constant values.

E. Kärkäs, Division of Geophysics, Dept. of Physical Sciences, University of Helsinki, Box 64, FI-00014 Finland, ekarkas@cc.helsinki.fi; T. Martma, Laboratory of Isotope Palaeoclimatology, Institute of Geology, Tallinn University of Technology, 7 Estonia Ave., EE-10143 Tallinn, Estonia; E. Sonninen, Radiocarbon Dating Laboratory, University of Helsinki, Box 64, FI-00014, Finland.

Ice sheets are the largest freshwater reservoirs on Earth and constitute a unique archive of past climate and environmental changes (e.g. Petit et al. 1999). Polar ice sheets and sea ice, with their high albedo, are important to the Earth's climate (Bindschadler 1998). Changes in mass balance of ice sheets have a pronounced effect on the global climate and sea level. Antarctica may be particularly important in this regard. Snow cover is very sensitive to climate change and has large feedback effect on the climate system due to the high albedo. Since snow covers almost all surfaces in Antarctica, small differences in albedo can mean large differences in absorbed radiation (Grenfell et al. 1994). The albedo is also spectrally distributed depending on grain size and shape, near-surface liquid water content, surface roughness, impurities and the angle of incidence of solar rays (Orheim & Lucchitta 1988). The properties of the surface snow give the continent its important climatic role and determine its energy and mass balance. To better understand these relationships it is essential to understand the annual snow accumulation rate and snow properties and their spatial variations.

Satellite remote sensing and large-scale numerical modelling allow us to study large and otherwise inaccessible areas. The physical properties of the snow surface are valuable ground truth data and can be used to validate remote sensing

measurements. Parameters such as albedo, snow grain size and surface temperature derived from remote sensing data are boundary conditions for various models (König et al. 2001). In radar mapping of snow cover, backscatter is determined by both surface and volume scattering; the former is dependent on the surface roughness and the dielectric properties of snow and the latter on the internal structure of snow including density, size and shape of the grains and the change in dielectric properties as controlled by impurities and water content. Solar radiation, wind packing and diurnal reversals of the temperature gradient influence the upper layers of snow. In dry snow the temperature gradient metamorphism associated with the transfer of water vapour is the main process for development of stratigraphic features (Colbeck 1983).

Coastal parts of western Dronning Maud Land are still largely unexplored. The European Project for Ice Coring in Antarctica (EPICA) is currently constructing a high-resolution climate record from the polar plateau (e.g. Sommer et al. 2000). The history of snow accumulation measurements in the western Maudheimvidda area of Dronning Maud Land (Fig. 1) is summarized by Isaksson & Karlén (1994a). Schytt (1958) had earlier performed detailed snow pit studies in the area. Recently, the Swedish Antarctic Research Programme (SWEDARP) and EPICA also performed snow accumulation and climate studies (Isaksson & Karlén 1994a, 1994b; Isaksson et al. 1996; Van den Broeke et al. 1999; Karlöf et al. 2000; Sommer et al. 2000). Snow distribution has also been examined and the results revealed the importance of obtaining more information of the spatial variations of snow (Richardson et al. 1997).

In the present study the most recent annual accumulation, physical properties and layered structure of the snow cover were examined. We present data on summertime surface snow conditions in western Dronning Maud Land. The field campaigns were undertaken during the austral summers of 1999/2000, 2000/01 and 2003/04 as part of the Finnish Antarctic Research Programme (FINNARP). The physical properties were measured also to provide ground truth data for comparison with optical measurements performed at the same time and for remote sensing applications.

Study area and methods

Most of the measurement sites were located on the small Riiser-Larsen ice shelf or on the Ritscherflya ice sheet between the Vestfjella and Heimefrontfjella mountain ranges, which run approximately parallel to the coast (Fig. 1). One site was south of Heimefrontfjella on the polar plateau (site 17). Snow on the Kvitkuven ice rise (site 2) and Högisen ice dome (site 11) was also investigated. These local topographic features are exceptions in the area, where otherwise the elevation increases with increasing distance from the coast (Kärkäs et al. 2002). The coastal area is more affected by the changing sea ice cover and cyclonic activity than high elevation areas (King & Turner 1997). The near-surface climate in Dronning Maud Land is determined by a combination of predominant katabatic winds and synoptic winds forced by transient cyclones travelling eastwards parallel to the coastline (Reijmer 2001). The intense cyclonic storms from the Weddell Sea play an important role in the snow accumulation (Noone et al. 1999). According to Reijmer (2001) mean air temperatures in the area are –20 °C on the ice shelf, –17 °C behind the grounding line and –21 °C near Heimefrontfjella.

A total of 17 snow pit sites were studied in 1999/2000, 11 pits in 2000/01 and 10 sites in 2003/04 (Table 1). The location of the Finnish research station and the navigable traverse routes determined the measurement sites. Kvitkuven and Högisen were selected because of their lower backscattering observed in the RADARSAT imagery (Fig. 1). The geographic positions of the snow measurement sites were determined with a Garmin hand-held global positioning system instrument with a precision of ± 100 m or better.

Measurements were conducted in situ in shallow snow pits (1 - 2 m) and consisted of profiles at 2 - 10 cm intervals of visible stratigraphy, temperature, density, grain size and shape, dielectric constant and wetness. Samples were collected to determine conductivity, pH and oxygen isotope ratio ($\delta^{18}O$). The measurement methods are described in detail in Rasmus et al. (2003). Snow density was measured using a cylinder sampling kit with a volume of 0.5 dm^3 (Ø 6 cm) in 1999/2000 and 0.25 dm^3 (Ø 5 cm) in 2000/01 and 2003/04, and a spring balance with an accuracy of $\pm 10^{-3}$ kg. Snow grains were photographed in the field using a special camera stand (Pihkala & Spring 1985) and classified according to Colbeck

et al. (1990). The reported snow grain size is the greatest extension of grain (Colbeck et al. 1990; Gay et al. 2002). The grain sizes were determined from digital images using image processing software (ImageJ). A total of 760 images and 13 460 grains were analysed.

The relative dielectric constant of a medium ε is complex and consists of a real (ε′) and an imaginary part (ε″):

$$\varepsilon' = \varepsilon' - j\varepsilon''$$

where $j = \sqrt{-1}$. The term ε′ is usually referred to as the permittivity of the material and ε″ the dielectric loss factor (Ulaby et al. 1986). Here we consider only the real part and refer to it as the dielectric constant. In dry snow the imaginary part is negligible. The dielectric constant was measured with a TEL 051 dielectric probe (LEAS, Grenoble, France) in 1999/2000 and with the Finnish snow fork device in 2000/01 and 2003/04 (Sihvola & Tiuri 1986). The liquid water content (wetness) is expressed as a percentage by volume.

Conductivity, pH and $\delta^{18}O$ were analysed in melted samples. Conductivity was determined with Handylab LF 513 T (Schott Glas, Mainz, Germany) in 1999/2000 and 2000/01, and with CDM210 conductivity meter (MeterLab, Radiometer Analytical, France) in 2003/04. pH was determined with Handylab BlueLine 24 pH (Schott Glas, Mainz, Germany).

The $\delta^{18}O$ ratios for 1999/2000 and 2000/01 were analysed at the Institute of Geology, Tallinn University of Technology, using a Delta-E mass-spectrometer (Finnigan-MAT, Bremen, Germany) and for 2003/04 at the Radiocarbon Dating Laboratory, University of Helsinki, using Delta+XL mass spectrometer connected online to GasBench II (Thermofinnigan, Bremen, Germany). The samples were measured against laboratory internal reference waters, which were calibrated on the V-SMOW/SLAP scale. The reproducibility of replicate analyses is generally better than ±0.15‰.

The $\delta^{18}O$, density profiles and layering were examined to identify the annual layers and determine yearly accumulation. $\delta^{18}O$ profiles are commonly used to determine the annual accumulation in areas where there is enough solid precipitation both in winter and summer, since the local $\delta^{18}O$ maxima indicate the summer surfaces (Isaksson & Karlén 1994b).

Table 1. Snow pit site coordinates with elevation and distance from the coast. AWS refers to automatic weather stations in the area (Reijmer 2001) and snow pit sites close to them.

Site	Latitude	Longitude	Approx. elevation (m a.s.l)	Distance from coast (km)
1	72° 32.0' S	16° 34.0' W	30	3
2	72° 36.6' S	16° 18.6' W	250	15
3a	72° 40.0' S	16° 41.9' W	55	20
3b	72° 45.0' S	16° 00.1' W	60	30
3c	72° 45.0' S	16° 30.0' W	60	25
4	72° 45.2' S	14° 18.3' W	70	70
5	72° 57.9' S	13° 34.7' W	270	110
6	73° 02.0' S	13° 19.5' W	250	120
7	73° 03.6' S	13° 21.8' W	250	120
8	73° 05.3' S	13° 20.2' W	240	120
9	73° 04.1' S	13° 28.2' W	235	120
10	73° 12.5' S	13° 13.0' W	375	140
11	73° 26.3' S	14° 26.7' W	990	130
12	73° 27.4' S	12° 33.3' W	905	170
13	73° 43.0' S	12° 18.6' W	930	195
14	74° 00.8' S	12° 01.1' W	980	230
15	74° 14.0' S	11° 48.0' W	1000	250
16	74° 28.7' S	11° 33.1' W	1100	275
17	74° 59.9' S	10° 00.5' W	2550	355
AWS4	72° 45.1' S	15° 30.0' W	60	45
AWS5	73° 06.2' S	13° 09.8' W	370	130
AWS6	74° 29.0' S	11° 31.2' W	1100	275

Results and discussion

Snow properties

Table 2 and Fig. 2 compile the results of the snow properties (surface temperature, temperature gradient between 30 and 100 cm depth, density, grain size, dielectric constant, liquid water content, conductivity, pH, $\delta^{18}O$ and accumulation) showing the mean values of the topmost metre and within the annual accumulation layer for the ice shelf, the coastal region and the plateau. Table 3 shows the correlations between the different mean values of accumulation year and elevation, distance to the ice edge and latitude.

The surface temperature decreased from the ice edge to the polar plateau and correlated best with elevation (Table 3). The season 2003/04 had the highest surface temperature values and the summer season was characterized by a heavy surface melting from the coast to site 10 behind the grounding line. The temperature profiles displayed diurnal fluctuations in the top 0.3 m. At night the temperature maxima were beneath the surface

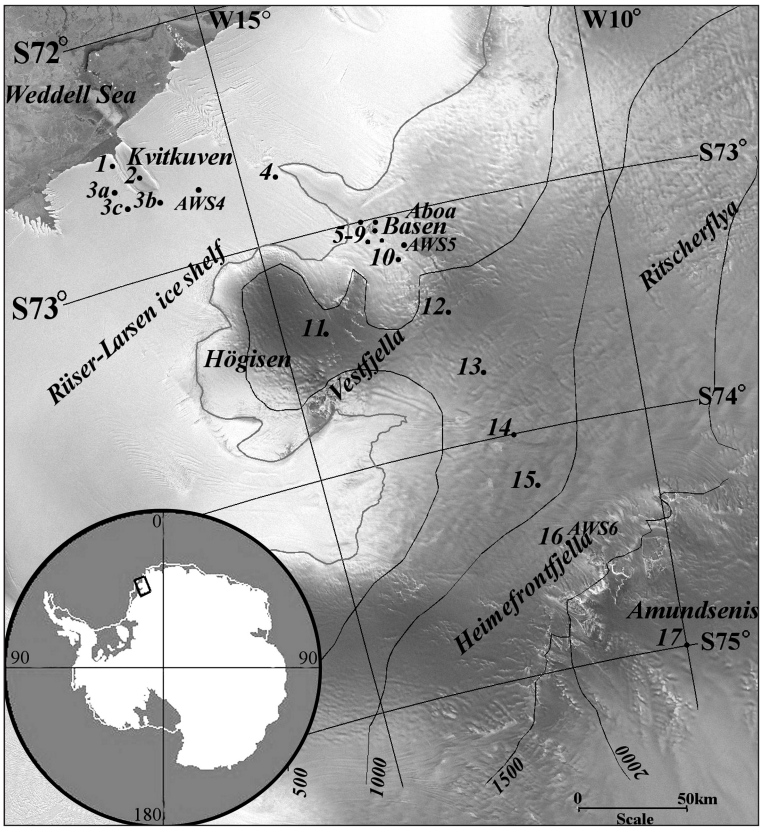

Fig. 1. Map of the measurement area in western Dronning Maud Land showing the locations of snow pit sites 1-17 and automatic weather station sites (AWS). The Finnish research station Aboa (73° 03' S, 13° 24' W) is located on the Basen nunatak at an elevation of 485 m a.s.l. Part of the RADARSAT mosaic (Jezek 1999; Jezek et al. 2002) was used as background (RADARSAT data © Canadian Space Agency 1997, used with permission).

due to colder air temperatures. However, the ability of solar radiation to penetrate into a snow cover, combined with the low thermal conductivity of snow, can lead to a sub-surface temperature maximum in daytime as well (Koh & Jordan 1995). The temperature distribution in the upper snow and firn layers is dominated by surface temperature variations, i.e. by upward or downward heat transfer, depending on the near-surface temperature gradient (Lange 1985). Temperature gradients in the snow affect snow grain evolution and therefore the optical properties of the snow pack

Table 2. The mean values and standard deviations of measured snow properties (surface temperature T_s, temperature gradient ΔT, density ρ, density given by snow fork ρ_f, grain size E, dielectric constant ε, wetness θ, conductivity κ, pH, number of layers, number of ice layers, $\delta^{18}O$ and accumulation (a) in the topmost metre of snow cover and (b) in the annual layer on the ice shelf, for the coastal region between the grounding line and Heimefrontfjella and on the plateau.

(a)	T_s (°C)	ΓT (°C)	ρ (kg m^{-3})	ρ_f (kg m^{-3})	E (mm)	ε	θ (vol %)	κ (μS cm^{-1})	pH	Layers	Ice layers
Shelf	–2.6±3.4	6.5±1.6	394±26	363±35	2.0±1.0	1.76±0.07	0.6±0.4	24.8±28.8	6.0±0.3	10±4	4±2
Coast	–4.0±3.5	–5.6±1.8	396±30	382±27	1.5±0.6	1.80±0.10	0.7±0.5	4.8±3.2	6.3±0.6	12±4	6±3
Plateau	–15.6±1.3	–6.5±0.8	367±22	324	1.3	1.65	0.3	2.4±0.1	6.4±0.1	16±4	10±2

(b)	ρ (kg m^{-3})	ρ_f (kg m^{-3})	E (mm)	ε	θ (vol %)	κ (μS cm^{-1})	pH	$\delta^{18}O$‰	Layers	Ice layers	Acc. (mm w.e.)
Shelf	388±28	362±36	2.0±1.0	1.75±0.08	0.6±0.4	34.3±40.6	6.0±0.3	–20.39±2.99	9±3	3±1	312±28
Coast	391±32	370±38	1.5±0.7	1.80±0.11	0.7±0.5	5.5±5.0	6.3±0.6	–26.03±3.94	8±3	4±2	215±43
Plateau	367±5	319	1.0	1.64	0.3	2.4±0.1	6.7±0.4	–37.87	5	3	92±25

Fig. 2. Spatial distributions of (a) mean annual values of $\delta^{18}O$, (b) accumulation, (c) conductivity and (d) grain size in 1999/2000, 2000/01 and 2003/04. The linear (a-b) and exponential (c-d) fit has been calculated, and the r value shows the Pearson correlation coefficient.

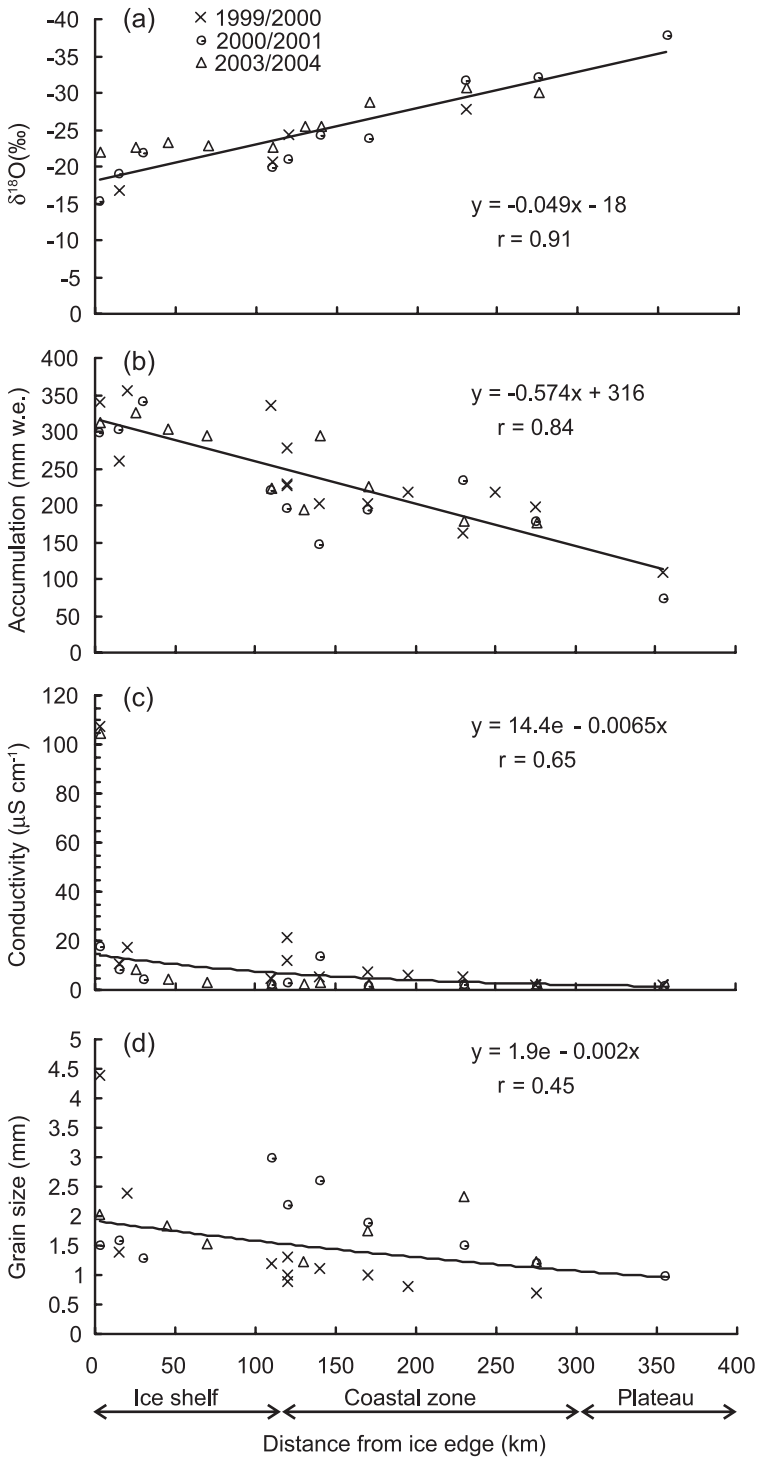

and they in turn affect the vertical distribution of absorbed energy (Brandt & Warren 1993).

Snow density is a very important variable for the dielectric constant and affects the signals detected with the ground penetrating radar and microwave remote sensing (Richardson et al. 1997). The mean snow densities of the annual layer were 408 kg m^{-3} (1999/2000), 367 kg m^{-3} (2000/01) and 385 kg m^{-3} (2003/04) in the area as a whole and ranged between 324 and 458 kg m^{-3}. Snow density values vary due to local meteorological conditions at different sites and the time of year when accumulation occurred. Density did not have any correlation with elevation, distance from the ice edge or latitude (Table 3), but was the lowest in the local topographic highs and on the plateau. Mean density of the topmost metre was 394 ± 26 kg m^{-3} on the ice shelf, 396 ± 30 kg m^{-3} in the coastal region and 367 ± 22 kg m^{-3} on the plateau. Oerter et al. (1999) found the values of 432 ± 21 kg m^{-3}, 387 ± 35 kg m^{-3} and 338 ± 12 kg m^{-3} for the same regions in the topmost 2 m. In the same ice shelf area Gjessing & Wold (1986) measured the lowest values on the inner half of the shelf and at the top of Kvitkuven; the highest values were at the grounding line and on the outer part of the shelf.

Table 3. The Pearson correlation coefficients between the mean annual value of the measured properties (surface temperature T_s, temperature gradient ΔT, density ρ, density given by snow fork ρ_f, grain size E, dielectric constant ε, wetness θ, conductivity κ, pH, $\delta^{18}O$, number of layers, number of thick ice layers and thin crusts, accumulation) and elevation, distance from the ice edge and site latitude. The values given in boldface have significance levels ≥95 %.

	Elevation	Distance	Latitude
Elevation	1		
Distance	**0.89**	1	
Latitude	**0.92**	**0.98**	1
T_s	**-0.71**	**-0.60**	**-0.62**
ΔT	0.03	0.00	-0.03
ρ	-0.22	-0.14	-0.17
ρ_f	-0.25	-0.08	-0.14
E	**-0.34**	**-0.40**	**-0.39**
ε	-0.27	-0.12	-0.20
θ	-0.15	-0.10	-0.12
κ	-0.31	**-0.44**	**-0.38**
pH	0.10	0.15	0.09
$\delta^{18}O$	**-0.87**	**-0.91**	**-0.92**
Layers	-0.08	-0.13	-0.11
Ice layers	0.07	0.08	0.09
Accumulation	**-0.79**	**-0.84**	**-0.80**

The density profiles in the topmost metre were highly variable, partly due to the development of intermittent layers of depth hoar and ice lenses. Density variations decreased with depth and the mean density increased, having a weak positive correlation with depth (r = 0.41). The increase of density with depth is usually most visible at depths greater than 4 - 5 m (West et al. 1996).

The liquid water content was the highest in 1999/2000 (0.9 volume %), although in 2003/04, surface melting was partly too heavy to be detected by snow fork. Microwave interaction with a snow cover is greatly influenced by the presence of liquid water and therefore conditions that can lead to an increase or decrease in snow wetness are of considerable interest to the radar remote sensing community (Koh & Jordan 1995). The effect of liquid water on snow albedo is to increase the effective grain size, because the refractive index contrast between water and ice is very small (Wiscombe & Warren 1980).

Conductivity values decreased exponentially with increasing distance from the ice edge (Fig. 2). Conductivity in melted samples reflects the conductivity of all ions present in the water (Hammer 1983). Site 1 at the edge of the ice shelf had much higher conductivity values in 1999/2000 and 2003/04 than the other ice shelf sites, probably due to remarkably high transport of sea salt. The high peaks in conductivity profiles seem to reflect individual storm events and occur in the area both during winter and summer. They cannot be used alone for accurate dating. Major sea salt depositions have previously been found to occur in coastal Antarctica both during the winter (Legrand & Mayewski 1997) and during the summer months (Aristarain & Delmas 2002). In the present study the southernmost sites had conductivity values similar to those found at the South Pole (2 - 3 μS cm^{-1}; Mosley-Thompson et al. 1985).

Snow grain size and shape

The mean grain size in the annual layer ranged between 1.5 and 1.8 mm. Grain size decreased exponentially with the distance from the ice edge (Fig. 2). The size distribution of all measured grains is seen in Fig. 3. The mean size of all measured grains was 1.3 (Fig. 3), in agreement with the coastal grain size of 0.7 - 1.2 mm measured along the traverse route to Dome Fuji Station

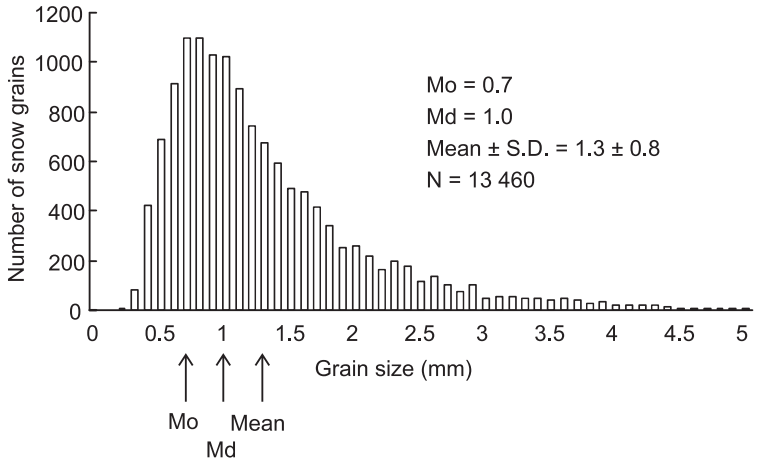

Fig. 3. Grain size distribution for the entire data set. Mode, median and mean values are given. Total number of processed snow grains was 13 460.

(Shiraiwa et al. 1996). In the interior of Antarctica, snow grain size has been found to be uniformly small; near the surface, fine grain size is surprisingly homogeneous over wide expanses (Gay et al. 2002). Aged snow in Antarctica can have significantly smaller grains at the surface due to the prevalence of wind drift (Grenfell et al. 1994).

For remote sensing applications, information of grain size is an important parameter. Especially in Antarctica, snow grain sizes have not been often measured and are fairly unknown (Gay et al. 2002). Larger grains result in more effective volume scattering and in lower passive microwave emissivity (Zwally 1977). Snow grain size is the most important variable controlling snow albedo (Brandt et al. 1991). The near infrared albedo is very sensitive to snow grain size and grain size normally increases as the snow ages, causing a reduction in albedo (Warren 1982). The growth of ice particles in dry snow is caused by diffusion of water vapour due to temperature gradients in the snow cover (Colbeck 1983). Grain size at any depth is dependent on both the temperature, which determines the rate of metamorphism, and the accumulation rate, which determines the age of the snow at that depth (Goodwin et al. 1994).

Typically the grains observed in our study were well rounded. Clustered poly-crystals were found at many sites and were included with the rounded grains. In total 4 % of all measured grains were partly decomposed precipitation crystals in the snow surface, 73 % were rounded grains, 11 % were faceted crystals, 9 % were depth hoar grains and 3 % were surface hoar according to the classification by Colbeck et al. (1990).

Dielectric constant

The mean liquid water content was less than 1 %. The snow cover could thus be considered dry and the imaginary part of the complex dielectric constant is negligible. The distance to the surface should be 5 cm to obtain reliable snow fork results. Here the snow fork results for the first 4 cm have been omitted. The mean values of dielectric constant in our measurements were between 1.7 and 1.8. This is in good agreement with the values obtained by Shiraiwa et al. (1996) for the coastal region.

The dielectric constant in snow and firn is affected by various physical and chemical parameters such as liquid water content, snow density, crystal fabric, conductivity, concentrations and compositions of ions and micro-particles (Richardson et al. 1997). However, the real part of the dielectric constant has been found to be almost solely dependent on the snow density and practically independent of the snow stratigraphy (Tiuri et al. 1984). The dielectric constant is also an important parameter in interpreting ground penetrating radar data and in microwave remote sensing. The dielectric constant of snow affects electromagnetic wave speed through snow and firn (Richardson et al. 1997).

Snow with divergent dielectric properties may form at the surface during periods with exceptional climatic or atmospheric conditions, such as intense storms, extremely high solar radia-

tion, high temperatures or atmospheric deposition of impurities (Richardson & Holmlund 1999). In Antarctica, dielectric properties of surface snow have seldom been measured (Shiraiwa et al. 1996). The strength of a backscattering signal reflected by a dry snow pack depends primarily on the dielectric properties, the number of internal reflectors and the grain size (Zahnen et al. 2002). In a perfectly homogeneous, dry snow pack without internal scatterers, snow reflectivity increases with the dielectric constant (Zahnen et al. 2002).

The manually measured densities ρ (in kg m^{-3}) were compared with the dielectric constant values. Results from 1999/2000, when dielectric constant was measured with the TEL 051 device gave a linear expression of:

$$\varepsilon = 0.0021\rho + 0.9617$$
$$r = 0.48$$

whereas the measurements from 2000/01 and 2003/04, obtained with the snow fork, led to the expression:

$$\varepsilon = 0.002\rho + 0.9904$$
$$r = 0.59$$

Our snow fork results are in good agreement with Shiraiwa et al. (1996; $\varepsilon = 0.0017\rho + 0.9597$ and Tiuri et al. (1984; $\varepsilon = 0.002\rho + 1$).

The relationship between the manually measured density ρ (kg m^{-3}) and the density obtained with the snow fork ρ_f forms a linear regression:

$$\rho_f = 1.03\rho - 6.62$$

The shape of grains could affect the measured dielectric constant. The snow fork was able to detect low-density depth hoar layers (Fig. 4). Our results show that those layers had lower dielectric constant values than rounded grains, although no linear correlation was found between snow grain size and delectric constant values.

Stratigraphy

Depth hoar layers were found usually under thin ice crusts (Fig. 4). Especially at greater distances from the coast, several depth hoar layers were found within a single accumulation year and those layers cannot be used alone to identify a summer surface in the measurement area, although the depth hoar layers were usually associated with summer surface as well (Fig. 4). Depth hoar in polar firn forms when large temperature gradients act on low-density firn (Alley 1988). At sites with low accumulation, only the annual depth hoar formed by mass loss to the atmosphere during the autumn may be recognizable, whereas at sites with high accumulation, like those in the present study (except site 17), individual storms may be preserved in the snow cover as a depth hoar layer (Alley 1988). If subjected to vapour transport down temperature gradients, buried low-density layers will develop into depth hoar, but high-density layers can develop into depth hoar only if they suffer significant mass loss to the free atmosphere in the upper 50 - 100 mm; this process seems to occur in the late summer or autumn (Alley 1988). At the South Pole, winter deposits have been found to be fine-grained and dense while the summer deposits are coarse-grained and less dense (Mosley-Thompson et al. 1985). In our measurement area the visible stratigraphy was more complex. Snow layering was better developed in coastal regions than on the polar plateau, as found in a previous study (Richardson et al. 1997). Figure 4 shows examples of stratigraphy at the site nearest to the coast (1), at the Kvitkuven ice rise (site 2) and at site 12 between two mountain ranges. Annual layers are determined from the $\delta^{18}O$ profiles. Conductivity values have high peaks during both winter and summer months. Depth hoar layers are found near the summer surface but are also visible during the whole accumulation year. Densities increase somewhat with the depth but values are quite constant within the topmost metre. Dielectric constant values vary considerably within the snow cover, clear evidence of the diverse small-scale layered structure.

Table 2 presents the mean number of visible layers and of ice layers within the topmost metre and the annual accumulation layer. Wet snow and summer melting conditions were observed at the seaward edge of the ice shelf during every season. Near the coast several thick ice layers (1 - 5 cm)

Fig. 4 (opposite page). Snow stratigraphy and measured snow profiles of density, dielectric constant grain size, conductivity and oxygen isotope ratio at (a) site 1 on the ice shelf in 2003/04, (b) site 2 on the Kvitkuven ice rise in 2000/01 and (c) site 12 between two coastal mountain ranges in 2000/01. Density measured with the snow fork is plotted with the dashed line in density profile, ice layers and crusts are marked with thick black lines and symbols of hoar layers are after Colbeck et al. (1990). Thin black lines distinguish different layers. Annual accumulation layers have been marked with thick dashed lines.

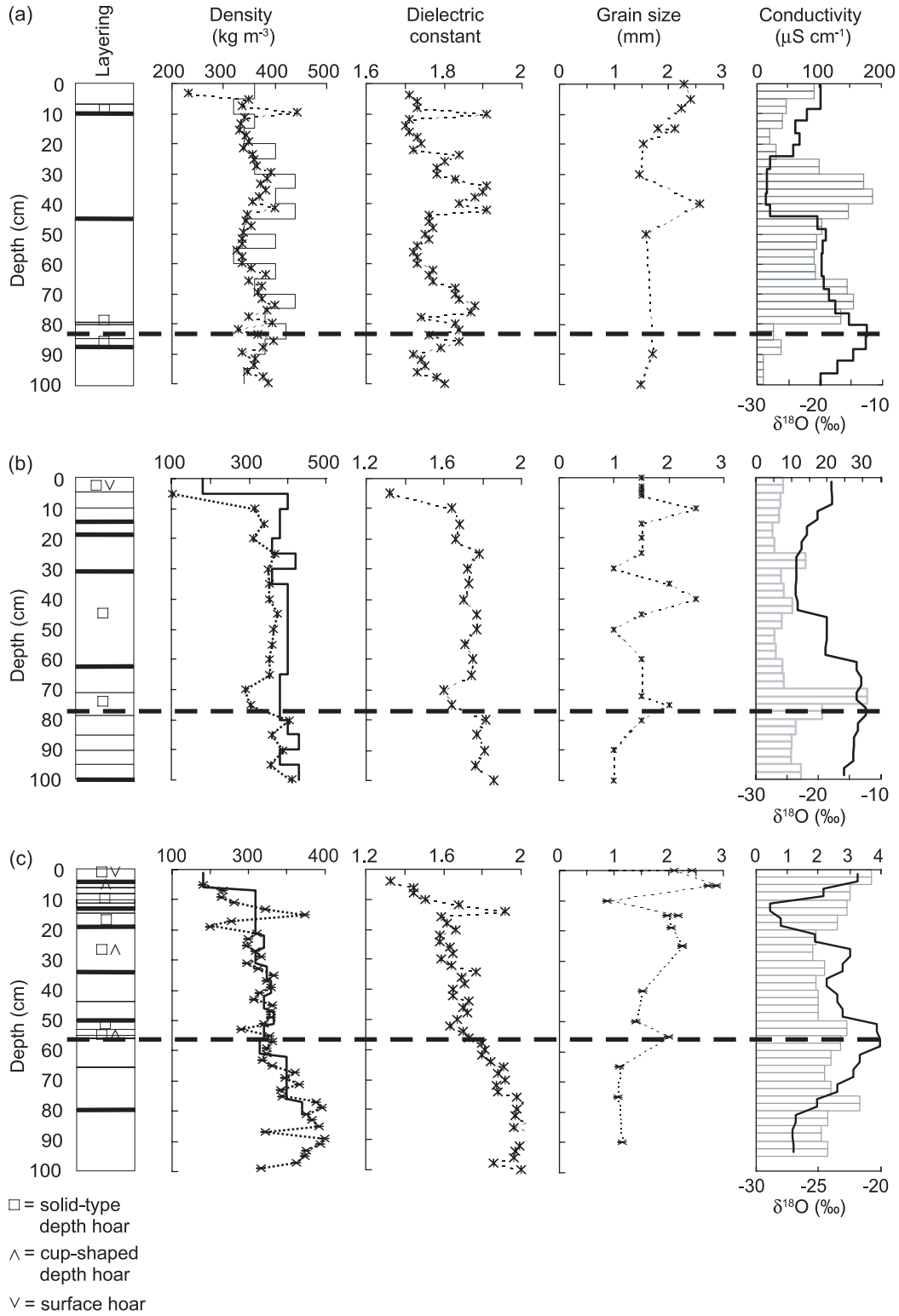
(a)
Layering
Density (kg m-3)
Dielectric constant
Grain size (mm)
Conductivity (µS cm-1)
Depth (cm)
δ18O (‰)
(b)
(c)
□ = solid-type depth hoar
∧ = cup-shaped depth hoar
∨ = surface hoar

were observed while behind the grounding line they were mostly thin ice crusts (1-2 mm). Ice crusts form due to solar radiation or wind during the hiatus in accumulation (Goodwin 1990). A total of 3-4 ice crusts were found in snow pit profiles for one accumulation year (Table 2). This is in agreement with Reijmer's (2001) observation showing 4-5 major accumulation events in the area per year. Rott et al. (1993) emphasized the importance of snow stratification in the interpretation of microwave remote sensing measurements. Highest backscattering coefficients and small angular variations have been observed for refrozen firn near the coast in Dronning Maud Land while pronounced stratification, including depth hoar layers, resulted in increased backscattering intensities (Rott et al. 1993). A large number of ice lenses, wind crusts or pronounced layer boundaries increases reflectivity (Zahnen et al. 2002). Heterogeneous snow pack should therefore appear brighter than homogeneous snow (Zahnen et al. 2002).

Snow on the local topographic highs, the Kvitkuven ice rise (site 2) and the Högisen ice dome (site 11), had notably lower densities and dielectric constants than nearby sites at lower elevations and had no thick ice layers, all of which may be an indication of locally reduced speed of the katabatic outflow.

The $\delta^{18}O$ values and annual accumulation

The mean annual $\delta^{18}O$ and accumulation values are presented in Table 2 for three different areas and in Table 4 for the separate snow pits. The isotope ratios have been used to determine the annual layers. The mean $\delta^{18}O$ values were the lowest in 2003/2004, even though the cold southernmost site was not sampled. This indicates that the annual temperatures were coldest in 2003 despite the fact that the summer surface temperatures were high. The mean differences between winter minimum and summer maximum with standard deviations were 10.43 ± 3.35 ‰ in 1999/2000, 11.05 ± 2.86 ‰ in 2000/01 and 14.26 ± 2.61 ‰ in 2003/2004. The mean annual $\delta^{18}O$ values were strongly correlated with the distance from the ice edge and with the latitude (Fig. 2, Table 3). In view of the vast size of the Antarctic ice sheet it is important to extend considerably the investigation of the distribution of the isotopic ratios in surface snow to provide a better documented data base for interpreting the isotopic profiles of deep ice cores and also for validating isotopic model results with present-day data (Qin et al. 1994).

Figure 5 shows how snow layering and $\delta^{18}O$ profiles varied at site 5 during three different accumulation years. The range of isotope values is similar in different years, indicating similar annual temperature variations, although the year 2003 seemed to be the coldest. The accumulation ranged between 219 and 335 mm w.e. due to annual differences in precipitation and also irregularity in wind redistribution. This site showed one of the largest variations in accumulation between the years (Table 4). Within one single site the accumulation values varied between 19 and 145 mm w.e. from year to year. Also the results from the different snow pits excavated during the same season at the same site (AWS sites) showed

Table 4. The annual values of $\delta^{18}O$ and accumulation (Acc.) for the years 1999, 2000 and 2003. Values marked in boldface have been obtained from the profile of the year 2000. For the AWS sites the mean values and standard deviations of four snow pits are shown.

Site	$\delta^{18}O$ 1999 (‰)	$\delta^{18}O$ 2000 (‰)	$\delta^{18}O$ 2003 (‰)	Acc. 1999 (mm w.e.)	Acc. 2000 (mm w.e.)	Acc. 2003 (mm w.e.)
1	–	–15.29	–21.76	339	297	311
2	–16.83	–18.95	–	259	301	–
3a	–	–	–	355	–	–
3b	–	–21.87	–	–	339	–
3c	–	–	–22.43	–	–	322
4	–	–	–22.80	–	–	292
5	–20.67	–19.82	–22.57	335	219	222
6	–	–	–	–	–	–
7	–	–	–	277	–	–
8	–24.49	–	–	229	–	–
9	–	–20.98	–	227	196	–
10	**–24.52**	–24.27	–25.29	203	148	293
11	–	–	–	–	–	–
12	–	–23.80	–28.58	203	194	223
13	–	–	–	218	–	–
14	–27.98	–31.67	–30.61	162	233	178
15	–	–	–	217	–	–
16	**–29.85**	–32.12	–	197	178	–
17	–	–37.87	–	109	74	–
AWS4			–23.19 ± 1.09			301 ± 13
AWS5			–25.39 ± 1.98			194 ± 5
AWS6			–29.86 ± 0.98			175 ± 19

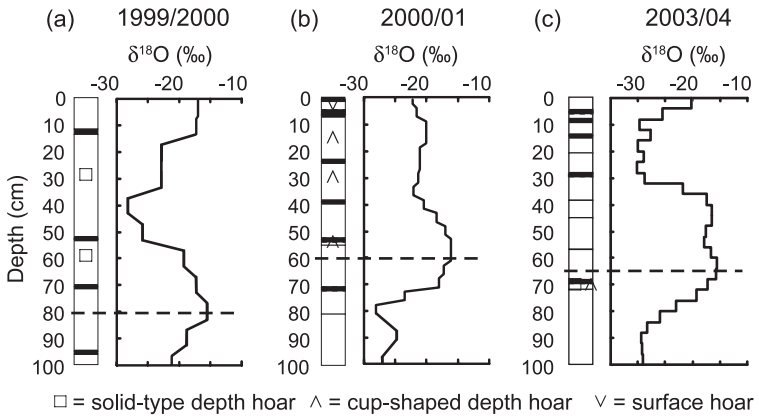

Fig. 5. Snow layering and oxygen isotope ratio profiles at site 5 in (a) 1999/2000, (b) 2000/01 and (c) 2003/04. Ice crusts are marked with the thick black lines and symbols of hoar layers are after Colbeck et al. (1990). Annual accumulation layers have been marked with dashed lines.

variations between 5 and 19 mm w.e. (Table 4). These temporal and spatial variations are partly due to redistribution of snow by winds. However, the accumulation rates clearly decreased with increasing distance from the coast and three geographical regions can be identified: ice shelf (sites 1-4), coastal region behind the grounding line (sites 5-16) and polar plateau (site 17). Accumulation values for the ice shelf and coastal region are lower than observed earlier in the same area (Isaksson & Karlén 1994a) but are close to values for the years 1998–2001 obtained from the automatic weather stations (Reijmer & Van den Broeke 2003). In the present study accumulation had the best correlation with the distance from the ice edge although there was good correlation also with the site latitude and elevation (Table 3).

Conclusions

The physical properties of the topmost metre of the snow cover were measured during the austral summers of 1999/2000, 2000/01 and 2003/04 in western Dronning Maud Land in the vicinity of the Finnish research station Aboa. Studies of spatial variations are important to reveal the representativeness of point measurements, for remote sensing applications and modelling studies. Some measured quantities (density, dielectric constant and pH) stayed fairly constant with the increasing distance from the ice edge and an elevation change from 30 to 2550 m a.s.l. Although there was no trend from the coast to inland for most of the properties, there was strong heterogeneity within any single site. This emphasizes the importance of spatial studies to better understand these variations.

Based on our results the snow properties differed between the geographical areas: (1) the ice shelf, (2) the coastal region and (3) the polar plateau. The Heimefrontfjella mountain range forms a steep step in the landscape and causes changes of the gradients of studied properties towards the plateau. In addition to these three snow zones, two sub-groups could be distinguished on the basis of the amount and thickness of the ice layers, grain sizes, density, conductivity and accumulation values. These sub-groups are: (4) local topographic highs and (5) the edge of the ice shelf. The local topographic highs had lower snow densities and dielectric constants, and the surface roughness and stratigraphy were not as well developed as at nearby sites at lower elevation. The site at the ice edge had abundant thick ice layers, large clustered snow crystals and high conductivity values relative to the rest of the ice shelf.

Conductivity values decreased exponentially with the distance from the ice edge. Snow temperature, conductivity, grain size, $\delta^{18}O$ ratio and accumulation rate had a clear decreasing trend from the ice edge to inland. Snow surface temperature correlated best with elevation, while grain size, conductivity and accumulation rate had the best (inverse) correlation with the distance from the ice edge. The $\delta^{18}O$ ratio correlated best with the site latitude. The mean accumulation was 316±29 mm w.e. on the ice shelf, 218±46 mm w.e. in the coastal region from the grounding line to Heimefrontfjella and 92±25 mm w.e. on the polar plateau.

Seasonal meteorological variations and their effects on snow metamorphism and microstratigraphy need to be investigated in greater detail.

This requires sampling and measuring at higher resolution. In future studies, it would be interesting to make detailed measurements of the snow on nunataks, where there is strong summer melting and evaporation.

Acknowledgements.—The Academy of Finland financed the Seasonal Snow in Antarctica project (nos. 43925 and 54086 to M. Leppäranta). Logistics were provided by FINNARP. We are grateful to Toikka Oy (www.toikkaoy.com) for providing the snow fork. We appreciate the helpful comments of E. Isaksson and M. Leppäranta. We would like to thank H. B. Granberg, C. Lavoie, K. Rasmus, K. Kanto, O.-P. Mattila, O. Ruohoniemi and T. Hämäläinen for their help during the fieldwork and analyses.

References

Alley, R. B. 1988: Concerning the deposition and diagenesis of strata in polar firn. *J. Glaciol. 34*, 283–290.

Aristarain, A. J. & Delmas, R. J. 2002: Snow chemistry measurements on James Ross Island (Antarctic Peninsula) showing sea-salt aerosol modifications. *Atmos. Environ. 36*, 765–772.

Bindschadler, R. 1998: Monitoring ice sheet behavior from space. *Rev. Geophys. 36*, 79–104.

Brandt, R. E., Grenfell, T. C. & Warren, S. G. 1991: Optical properties of snow. *Antarct. J. U.S. 26*, 272–275.

Brandt, R. E. & Warren, S. G. 1993: Solar-heating rates and temperature profiles in Antarctic snow and ice. *J. Glaciol. 39*, 99–110.

Colbeck, S. C. 1983: Theory of metamorphism of dry snow. *J. Geophys. Res. 88*, 5475–5482.

Colbeck, S., Akitaya, E., Armstrong, R., Gubler, H., Lafeuille, J., Lied, K., McClung, D. & Morris, E. 1990: The international classification for seasonal snow on the ground. International Commission on Snow and Ice. Wallingford, Oxon: International Association of Scientific Hydrology.

Gay, M., Fily, M., Genthon, C., Frezzotti, M., Oerter, H. & Winther, J.-G. 2002: Snow grain-size measurements in Antarctica. *J. Glaciol. 48*, 527–535.

Gjessing, Y. & Wold, B. 1986: Absolute movements, mass balance and snow temperatures of the Riiser-Larsenisen Ice Shelf, Antarctica. *Nor. Polarinst. Skr. 187*, 23–31.

Goodwin, I. D. 1990: Snow accumulation and surface topography in the katabatic zone of Eastern Wilkes Land, Antarctica. *Antarct. Sci. 2*, 235–242.

Goodwin, I. D., Higham, M., Allison, I. & Jaiwen, R. 1994: Accumulation variations in eastern Kemp Land, Antarctica. *Ann. Glaciol. 20*, 202–206.

Grenfell, T. C., Warren, S. G. & Mullen, P. C. 1994: Reflection of solar radiation by the Antarctic snow surface at ultraviolet, visible, and near-infrared wavelengths. *J. Geophys. Res. 99(D9)*, 18669–18684.

Hammer, C. U. 1983: Initial direct current in the build-up of space charges and the acidity of ice cores. *J. Phys. Chem. 87*, 4099–4103.

Isaksson, E. & Karlén, W. 1994a: Spatial and temporal patterns in snow accumulation, western Dronning Maud Land, Antarctica. *J. Glaciol. 40*, 399–409.

Isaksson, E. & Karlén, W. 1994b: High resolution climatic information from short firn cores, western Dronning Maud Land, Antarctica. *Clim. Chang. 26*, 421–434.

Isaksson, E., Karlén, W., Gundestrup, N., Mayewski, P., Whitlow, S. & Twickler, M. 1996: A century of accumulation and temperature changes in Dronning Maud Land, Antarctica. *J. Geophys. Res. 101(D3)*, 7085–7094.

Jezek, K. C. 1999: Glaciologic properties of the Antarctic ice sheet from spaceborne synthetic aperture radar observations. *Ann. Glaciol. 29*, 286–290.

Jezek, K. & RAMP Product Team 2002: *RAMP AMM-1 SAR image mosaic of Antarctica*. Digital media. Fairbanks, AK: Alaska Satellite Facility, and Boulder, CO: National Snow and Ice Data Center.

Kärkäs, E., Granberg, H. B., Lavoie, C., Kanto, K., Rasmus, K. & Leppäranta, M. 2002: Physical properties of the seasonal snow cover in Dronning Maud Land, East-Antarctica. *Ann. Glaciol. 34*, 89–94.

Karlöf, L., Winther, J.-G., Isaksson, E., Kohler, J., Pinglot, J. F., Wilhelms, F., Hansson, M., Holmlund, P., Nyman, M., Petterson, R., Stenberg, M., Thomassen, M. P. A., Van der Veen, C. & Van de Wal, R. S. W. 2000: A 1500 year record of accumulation at Amundsenisen western Dronning Maud Land, Antarctica, derived from electrical and radioactive measurements on a 120 m ice core. *J. Geophys. Res. 105 (D10)*, 12471–12483.

King J. C. & Turner, W. M. 1997: *Antarctic meteorology and climatology*. New York: Cambridge University Press.

Koh, G. & Jordan, R. 1995: Sub-surface melting in a seasonal snow cover. *J. Glaciol. 41*, 474–482.

König, M., Winther, J.-G. & Isaksson, E. 2001: Measuring snow and glacier ice properties from satellite. *Rev. Geophys. 39*, 1–27.

Lange, M. A. 1985: Measurements of thermal parameters in Antarctic snow and firn. *Ann. Glaciol. 6*, 100–104.

Legrand, M. & Mayewski, P. 1997: Glaciochemistry of polar ice cores: a review. *Rev. Geophys. 35*, 219–243.

Mosley-Thompson, E., Kruss, P. D., Thompson, L. G., Pourchet, M. & Grootes, P. 1985: Snow stratigraphic record at South Pole: potential for paleoclimatic reconstruction. *Ann. Glaciol. 7*, 26–33.

Noone, D., Turner, J. & Mulvaney R. 1999: Atmospheric signals and characteristics of accumulation in Dronning Maud Land, Antarctica. *J. Geophys. Res. 104(D16)*, 19191–19211.

Oerter, H., Graf, W., Wilhelms, F., Minikin, A. & Miller, H. 1999: Accumulation studies on Amundsenisen, Dronning Maud Land, Antarctica, by means of tritium, dielectric profiling and stable-isotope measurements: first results from the 1995-96 and 1997-97 field seasons. *Ann. Glaciol. 29*, 1–9.

Orheim, O. & Lucchitta, B. K. 1988: Numerical analysis of Landsat thematic mapper images of Antarctica: surface temperatures and physical properties. *Ann. Glaciol. 11*, 109–120.

Petit, J. R., Jouzel, J., Raynaud, D., Barkov, N. I., Barnola, J.-M., Basile, I., Bender, M., Chappellaz, J., Davis, M., Delaygue, G., Delmotte, M., Kotlyakov, V. M., Legrand, M., Lipenkov, V. Y., Lorius, C., Pépin, L., Ritz, C., Saltzman, E. & Stievenard, M. 1999: Climate and atmospheric history of the past 420,000 years from the Vostok ice core, Antarctica. *Nature 399*, 429–436.

Pihkala, P. & Spring, E. 1985: *A practical method for photographing snow samples. Rep. Ser. Geophys. 29*. Helsinki:

University of Helsinki, Division of Geophysics.
Qin, D., Petit, J. R., Jouzel, J. & Stievenard, M. 1994: Distribution of stable isotopes in surface snow along the route of the 1990 international trans-Antarctic expedition. *J. Glaciol. 40*, 107–118.
Rasmus, K., Granberg, H., Kanto, K., Kärkäs, E., Lavoie, C. & Leppäranta, M. 2003: *Seasonal snow in Antarctica data report. Rep. Ser. Geophys. 47.* Helsinki: University of Helsinki, Division of Geophysics.
Reijmer, C. H. 2001: *Antarctic meteorology. A study with automatic weather stations.* PhD thesis, University of Utrecht.
Reijmer, C. H. & Van den Broeke, M. R. 2003: Temporal and spatial variability of the surface mass balance in Dronning Maud land, Antarctica, as derived from automatic weather stations. *J. Glaciol. 49*, 512–520.
Richardson, C., Aarholt, E., Hamran, S.-E., Holmlund, P. & Isaksson, E. 1997: Spatial distribution of snow in western Dronning Maud Land, East Antarctica, mapped by a ground-based snow radar. *J. Geophys. Res. 102(B9)*, 20343–20353.
Richardson, C. & Holmlund, P. 1999: Spatial variability at shallow snow-layer depths in central Dronning Maud Land, East Antarctica. *Ann. Glaciol. 29*, 10–16.
Rott, H., Sturm, K. & Miller H. 1993: Active and passive microwave signatures of Antarctic firn by means of field measurements and satellite data. *Ann. Glaciol. 17*, 337–343.
Schytt, V. 1958: Glaciology II. Snow and ice temperatures in Dronning Maud Land. *Norwegian—British—Swedish Antarctic Expedition, 1949–52. Scientific Results IV*, 153-179.
Shiraiwa, T., Shoji, H., Saito, T., Yokoyama, K. & Watanabe, O. 1996: Structure and dielectric properties of surface snow along the traverse route from coast to Dome Fuji station, Queen Maud Land, Antarctica. *Proc. NIPR Symp. Polar Meteorol. Glaciol. 10*, 1–10. Tokyo: National Institute of Polar Research.
Sihvola, A. & Tiuri, M. 1986: Snow fork for field determination of the density and wetness profiles of a snow pack. *IEEE Trans. Geosci. Remote Sens. GE-24*, 717–720.
Sommer, S., Appenzeller, C., Röthlisberger, R., Hutterli, M. A., Stauffer, B., Wagenbach, D., Oerter, H., Wilhelms, F., Miller, H. & Mulvaney, R. 2000: Glacio-chemical study spanning the past 2 kyr on three ice cores from Dronning Maud Land, Antarctica. 1. Annually resolved accumulation rates. *J. Geophys. Res. 105(D24)*, 29411–29421.
Tiuri, M., Sihvola, A., Nyfors, E. & Hallikainen, M. 1984: The complex dielectric constant of snow at microwave frequencies. *IEEE J. Ocean. Eng. OE-9*, 377–382.
Ulaby, F. T., Moore, R. K. & Fung, A. K. 1986: *Microwave remote sensing, active and passive. Vol. 3. From theory to applications.* Reading, MA: Addison-Wesley Publishing Co.
Van den Broeke, M. R., Winther, J.-G., Isaksson, E., Pinglot, J. F., Karlöf, L., Eiken, T. & Conrads, L. 1999: Climate variables along a traverse line in Dronning Maud Land, East Antarctica. *J. Glaciol. 45*, 295–302.
Warren, S. G. 1982: Optical properties of snow. *Rev. Geophys. Space Phys. 20*, 67–89.
West, R. D., Winebrenner, D. P., Tsang, L. & Rott, H. 1996: Microwave emission from density-stratified Antarctic firn at 6 cm wavelength. *J. Glaciol. 42*, 63–76.
Wiscombe, W. J. & Warren, S. G. 1980: A model of spectral albedo of snow. I. Pure snow. *J. Atmos. Sci. 37*, 2712–2733.
Zahnen, N., Jung-Rothenhäusler, F., Oerter, H., Wilhelms, F. & Miller, H. 2002: Correlation between Antarctic dry snow properties and backscattering characteristics in RADARSAT SAR imagery. *EARSeL eProceedings 2*, 140–148.
Zwally, H. J. 1977: Microwave emissivity and accumulation rate of polar firn. *J. Glaciol. 18*, 195–215.